Published OnlineFirst December 19, 2013; DOI: 10.1158/1535-7163.MCT-13-0633

The Effect of Photoimmunotherapy Followed by Liposomal Daunorubicin in a Mixed Tumor Model: A Demonstration of the Super-Enhanced Permeability and Retention Effect after Photoimmunotherapy

Kohei Sano, Takahito Nakajima, Peter L. Choyke, and Hisataka Kobayashi

Abstract

In general, *de novo* solid tumors are composed of phenotypically and functionally heterogeneous malignant cells. This heterogeneity interferes with the effectiveness of targeted molecular cancer therapies. Even if most of the tumor is killed by a targeted treatment, recurrences are common and can be lethal. In this study, a mixed tumor model, which is predominantly a population of epidermal growth factor receptor (EGFR)-positive A431 cells combined with a smaller population of EGFR-negative Balb3T3/DsRed cells, was established. This mixed tumor was then treated with photoimmunotherapy, a newly developed target-cell–selective cancer therapy using a monoclonal antibody (mAb)–photosensitizer (IR700 fluorescence dye) conjugate and exposure of near-infrared light. Although photoimmunotherapy successfully treated EGFR-positive A431 cells in the mixed tumor, EGFR-negative Balb/DsRed cells were not responsive. However, photoimmunotherapy also induced a large increase in tumor permeability, known as the super-enhanced permeability and retention (SUPR) effect, which allowed a 5-fold increase in the accumulation of a liposomal chemotherapy (DaunoXome) and resulted in more effective therapy than either photoimmunotherapy or liposomal daunorubicin alone. The liposomal daunorubicin, administered 1 hour after EGFR-targeted photoimmunotherapy, was homogeneously distributed, allowing delivery to tiny surviving nests of EGFR-negative Balb3T3/DsRed cells, resulting in prolonged survival of mice. *Mol Cancer Ther; 13(2); 426–32. ©2013 AACR.*

Introduction

Solid tumors are composed of phenotypically and functionally heterogeneous malignant cells (1, 2), which arise from genetic (3) or epigenetic changes (4), or are a response to local environmental stresses such as hypoxia (5). Heterogeneity interferes with the effectiveness of cancer therapies, especially when targeted molecular therapies are employed. Even if most of the tumor is killed by a targeted treatment, recurrences are common and can be lethal.

Studying tumor heterogeneity in animal models is difficult. A fundamental limitation of most implanted cell lines is that are much less heterogeneous than *de novo* lesions and, therefore, do not reflect this common and important characteristic of spontaneous cancers. Transgenic mouse cancer models, can simulate cancers in patients better than any other models, attempt to overcome this problem; however, the variable timing for establishing a tumor make transgenic models inefficient and expensive to work with. Another approach is to use actual intact tumor explants; however, it is difficult to get uniform results across a population of animals because every explants is unique. Thus, there is a need for simpler tumor models that take into account tumor heterogeneity but are reproducible, efficient, and less costly than transgenic or explant models.

In this work, a mixed tumor model, which is predominantly a population of epidermal growth factor receptor (EGFR)-positive cells combined with a smaller population of EGFR-negative cells, was established. This mixed tumor was then treated with photoimmunotherapy, a newly developed cancer therapy using a monoclonal antibody (mAb)–photosensitizer (IR700 fluorescence dye) conjugate (6). Immediate and massive necrotic cell death is commonly seen only in target expressing cancer cells after exposure to near-infrared light. Following photoimmunotherapy the tumor demonstrates dramatically increased permeability (a phenomenon termed super-enhanced permeability and retention, SUPR) for nano-sized anticancer drugs, including liposomal daunorubicin, which further enhances killing of cancer cells. Because photoimmunotherapy is so specific for the targeted cell, with virtually no bystander effect, it is ideal to study in a multicell line tumor model. In this study, we investigate the effect of photoimmunotherapy in a tumor model in which two cell lines are mixed and implanted. We then

Authors' Affiliation: Molecular Imaging Program, Center for Cancer Research, National Cancer Institute, NIH, Bethesda, Maryland

Corresponding Author: Hisataka Kobayashi, Molecular Imaging Program, Center for Cancer Research, National Cancer Institute, NIH, Building 10, Room B3B69, 10 Center Drive, MSC1088, Bethesda, MD 20892-1088. Phone: 301-435-4086; Fax: 301-402-3191; E-mail: kobayash@mail.nih.gov

doi: 10.1158/1535-7163.MCT-13-0633

Published OnlineFirst December 19, 2013; DOI: 10.1158/1535-7163.MCT-13-0633

investigate the effect of liposomal daunorubicin on the cells remaining after effective photoimmunotherapy has been delivered.

Materials and Methods

Reagents

A water-soluble, silicon–phthalocyanine derivative, IRDye 700DX NHS ester (IR700) was purchased from LI-COR Biosciences. Panitumumab, a fully humanized immunoglobulin G_2 mAb directed against extracellular domain of the human EGFR 1 (HER1), was purchased from Amgen. Liposomal daunorubicin (DaunoXome) was purchased from Galen US Inc. All other chemicals used were of reagent grade.

Cells

EGFR-expressing A431 cells and Balb3T3/DsRed (Balb/DsRed) cells (7, 8) were used for photoimmunotherapy. A431, which is a human epidermoid carcinoma cell line (9), and Balb3T3, which is a virally transformed mouse 3T3 embryonic fibroblast cell line by virus infection, were purchased from American Type Culture Collection. Balb3T3 was transfected *pDsRed*-Express vector (Clonetech) in house. Cells were grown in RPMI-1640 supplemented with 10% FBS and 1% penicillin/streptomycin in tissue culture flasks in a humidified incubator at 37°C in an atmosphere of 95% air and 5% carbon dioxide. Both cells have been passaged in our laboratory within 4 months.

Synthesis of panitumumab–IR700 conjugates

Conjugation of panitumumab with IR700 was performed according to the procedure reported previously. In brief, panitumumab (1 mg, 6.8 nmol) was incubated with IR700 (66.8 μg, 34.2 nmol) in 0.1 mol/L aqueous Na_2HPO_4 (pH 8.6) at room temperature for 1 hour. The mixture was purified with a Sephadex G50 column (PD-10; GE Healthcare). The number of IR700 per mAb was approximately four.

Animal models

All *in vivo* procedures were carried out in compliance with the Guide for the Care and Use of Laboratory Animal Resources (1996), U.S. National Research Council, and approved by the National Cancer Institute/NIH Animal Care and Use Committee (Bethesda, MD). Six- to 8-week-old female homozygote athymic nude mice were purchased from the Charles River Laboratories (National Cancer Institute, Frederick, MD). The mixture of A431 (1×10^6) and Balb/DsRed cells (1×10^4) was injected subcutaneously in the right and left dorsi under isoflurane anesthesia, and the experiments were conducted 3 to 5 days after cell injection. To investigate the population of $EGFR^+$ tumor cells before and after photoimmunotherapy, mice were initially injected with panitumumab–IR700 (100 μg) intravenously, and 1 day later, the tumor was irradiated with near-infrared light from a red light-emitting diode at wavelengths of 670 to 710 nm and a power density of 50 J/cm^2, as measured with an optical power meter (PM 100; Thorlabs), and the photoimmunotherapy-treated tumors were excised and frozen 0, 1, and 7 days after photoimmunotherapy. Panitumumab–IR700 was reinjected at the same dose on day 6 after photoimmunotherapy and before tissue harvesting on day 7. Of note, 10-μm-thick frozen sections were prepared and fluorescence was assessed using an Olympus BX61 microscope (Olympus America, Inc.) equipped with the following filters: excitation wavelength 590 to 650 nm and 480 to 550 nm, emission wavelength 662.5 to 747.5 nm, and 590 nm long-pass for IR700 and DsRed, respectively. Transmitted light differential interference contrast images were also acquired. Furthermore, to evaluate histologic changes after photoimmunotherapy with near-infrared light, the tumors (A431 + Balb/DsRed) treated with photoimmunotherapy by exposing 0 and 50 J/cm^2 of near-infrared light were harvested in 10% formalin 1 hour after photoimmunotherapy. Serial three 10-mm slice sections were fixed on a glass slide with hematoxylin and eosin (H&E) staining.

In vivo fluorescence imaging studies after photoimmunotherapy

Five days after cell injection, 100 μg of panitumumab–IR700 was administered intravenously, and 1 day later, one tumor was irradiated with near-infrared light (50 J/cm^2), whereas the other side was shielded from light using aluminum foil. One hour after photoimmunotherapy, liposomal daunorubicin (DaunoXome; 30 mg/kg) was injected intravenously, and *in vivo* fluorescence images were obtained with a Maestro Imager (CRi) using a band-pass filter from 503 to 555 nm (excitation) and a long-pass green filter over 580 nm (emission). The tunable emission filter was automatically stepped in 10 nm increments from 500 to 800 nm for the green filter sets at constant exposure. The spectral fluorescence images consist of autofluorescence spectra and the spectra from daunorubicin, which were then unmixed, based on the characteristic spectral pattern of daunorubicin, using commercial software (Maestro software; CRi). Regions of interest were manually drawn on both tumors and the normal back of the mouse, and the fluoresence intensity was calculated. The tumors were excised and frozen for fluorescence microscopy. The fluorescence was assessed using an Olympus BX61 microscope equipped with the following filters: excitation wavelength 590 to 650 nm, 480 to 550 nm, and 480 to 550 nm, emission wavelength 662.5 to 747.5 nm, 590 nm long-pass, and 590 nm long-pass for IR700, DsRed, and daunorubicin, respectively. Spectral data of different reagents were separated using Maestro software (CRi). Transmitted light differential interference contrast images were also acquired.

In vivo therapeutic studies based on the SUPR effect

The mixed tumor cells (A431 and Balb/DsRed) were injected subcutaneously in the right flank of the mice. To determine the tumor volume, the greatest longitudinal diameter (length) and the greatest transverse diameter (width) were determined with an external caliper. Tumor

Published OnlineFirst December 19, 2013; DOI: 10.1158/1535-7163.MCT-13-0633

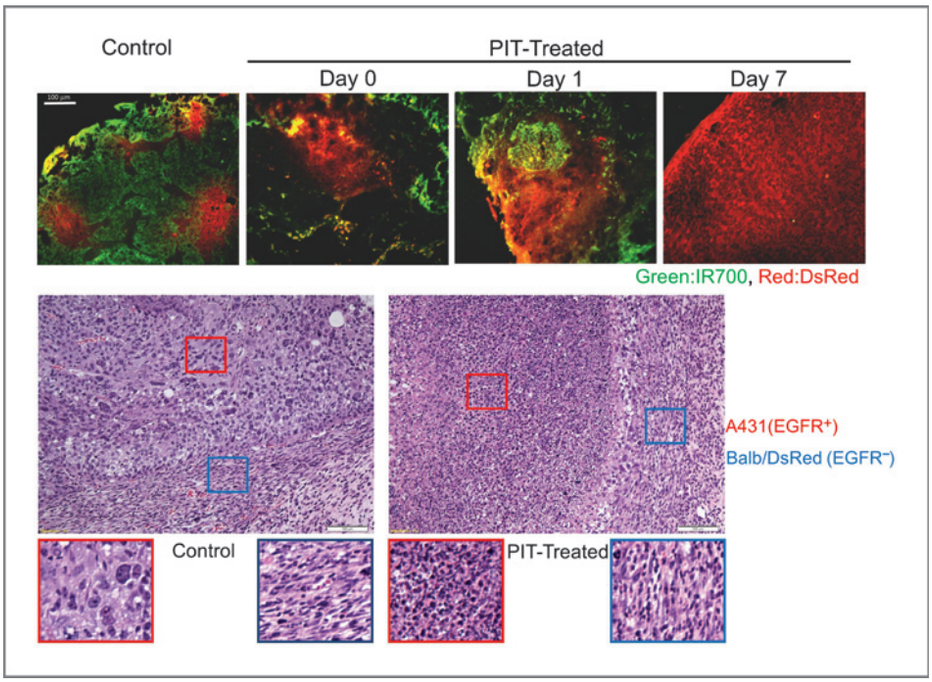

Figure 1. The mixed tumor model composed of EGFR-positive (A431) and EGFR-negative (Balb/DsRed) tumor cells. Panitumumab (Pan)–IR700 (green) was intravenously injected 1 day before photoimmunotherapy (PIT). Scattered Balb/DsRed tumor foci (red) were observed in A431 cells (green) before PIT. After PIT, severe damage was shown only in EGFR-positive A431 tumors, and the proportion of Balb/DsRed increased with time after PIT. Balb/DsRed cells eventually almost replaced the entire tumor at 7 days after PIT. Histologic evaluation before and after PIT. EGFR-targeted PIT induced selective intense necrosis of EGFR-positve A431 cells as indicated by H&E staining. In contrast, spindle-shaped Balb/DsRed cells remain intact even after PIT.

volume based on caliper measurements was calculated using the following formula: tumor volume = length$\times$ width^2 $\times$ 0.5 (8). Tumors reaching approximately 40 mm^3 in volume were selected for the study. Selected mice were randomized into four groups of at least 10 mice per group for the following treatments: (i) no treatment; (ii) daunorubicin (6 mg/kg) alone; (iii) photoimmunotherapy (50 J/cm^2) alone; (iv) photoimmunotherapy (50 J/cm^2) followed by liposomal daunorubicin (6 mg/kg) 1 hour later. After treatment, the mice were monitored daily, and their tumor volume was measured twice a week until it reached 1,300 mm^3, at which time mice were euthanized with carbon dioxide gas.

Statistical analysis

Data are expressed as means $\pm$ SEM from a minimum of three experiments, unless otherwise indicated. Statistical analyses were carried out using a statistics program (Statview). For multiple comparisons, a one-way ANOVA followed by the Tukey–Kramer test was used. The cumulative probability of survival, determined herein as the tumor volume failing to reach 1,300 mm^3, was estimated in each group with the use of the Kaplan–Meier survival curve analysis, and the results were compared with the log-rank test with Bonferroni correction for multiple comparisons. A P value of <0.05 was considered to indicate a statistically significant difference.

Results

Establishment of mixed tumor model

Inoculation of the mixture of A431 and Balb/DsRed cells produced tumors in which the majority of the cells were derived from EGFR$^+$ A431 cells, whereas small islands of Balb/DsRed cells became visible 3 to 5 days after innoculation (Fig. 1). Panitumumab–IR700 specifically accumulated in regions of DsRed-negative A431 tumor cells. Near-infrared light exposure induced immediate and massive necrosis of A431 cells but did not affect EGFR-negative Balb/DsRed cells (Fig. 1). As a consequence the proportion of Balb/DsRed cells in the tumors gradually increased as a function of time after EGFR-targeted photoimmunotherapy, and by 7 days the tumor was completely dominated by Balb/DsRed cells (Fig. 1).

In vivo dynamic fluorescence imaging after photoimmunotherapy

To evaluate the increased delivery of liposomal daunorubicin into tumors following photoimmunotherapy, commercially available liposomal daunorubicin (DaunoXome; mean diameter, 50 nm) was administered 1 hour after treatment with EGFR-targeted photoimmunotherapy. On the basis of the inherent fluorescence of daunorubicin, optical imaging showed that DaunoXome rapidly accumulated and diffused into photoimmunotherapy-treated tumors within 30 minutes after injection but not into untreated tumors (Fig. 2A and B). The ratios of fluorescence signal intensity at 30 minutes were 5-fold higher in the photoimmunotherapy-treated tumor compared with the control tumor using the equation $[(SI_{\text{photoimmunotherapy at 30 min}} - SI_{\text{Background at 30 min}})/(SI_{\text{Control at 30 min}} - SI_{\text{Background at 30 min}})]$ (Fig. 2C). IR700 fluorescence in photoimmunotherapy-treated tumor decreased due to washing out the antibody–IR700 conjugate from killed tumor cells and photobleaching (Fig. 2A). DaunoXome was widely distributed throughout the tumor, including those areas occupied by Balb/DsRed cells (Fig. 2D).

Published OnlineFirst December 19, 2013; DOI: 10.1158/1535-7163.MCT-13-0633

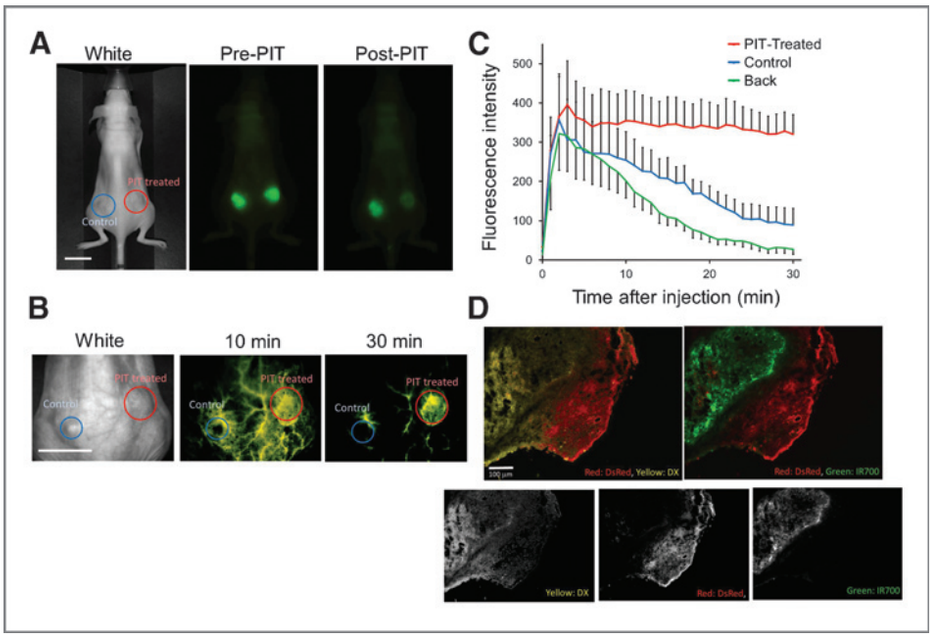

Figure 2. Enhanced delivery of liposomal daunorubicin based on PIT-induced SUPR effects. A, *in vivo* fluorescence images of Pan-IR700 (green). PIT was performed only on the right-side tumor with the left-side tumor serving as a control. B, liposomal daunorubicin (yellow) preferentially accumulated in PIT-treated mixed tumors (red circles) at 30 minutes after injection of liposomal daunorubicin, but did not accumulate in no near-infrared light exposure control tumors (blue circles) growing in the same mice. C, dynamic fluorescence intensity curves show that daunorubicin accumulated and was retained by PIT-treated tumors selectively. "Back" indicates the fluorescence in the back representing background signal. Data, means ± SEM ($n = 3$). D, intratumoral distribution of daunorubicin. Daunorubicin was broadly and homogeneously distributed post-PIT encircling the surviving tumor cells (Balb/DsRed and A431). DsRed, red; DaunoXome (DX; daunorubicin), yellow; IR700, green. Scale bars, 100 μm.

Therapeutic studies

A431 tumors were treated with a single dose of light (50 J/cm^2) 1 day after injection of panitumumab–IR700. We compared the efficacy of treatment in four groups of mice bearing mixed A431 and Balb/DsRed tumors ($n \geq 10$ in each group). All treated tumors had a volume of less than 1,300 mm^3, in accordance with the animal care and use guidelines of our institution. All but 5 mice were euthanized when their tumors exceeded 1,300 mm^3. Tumor volume was significantly reduced when treated with the combination of photoimmunotherapy and DaunoXome, compared with untreated control mice or mice treated with DaunoXome or photoimmunotherapy alone (Fig. 3A), and survival was significantly prolonged in mice with the combination therapy of photoimmunotherapy and DaunoXome compared with all other groups (Fig. 3B).

Discussion

Photoimmunotherapy, using panitumumab–IR700, showed a robust therapeutic effect on EGFR-expressing A431 tumor cells, whereas EGFR-negative tumor cells (Balb/DsRed) remained viable and eventually became the dominant cell type. Photoimmunotherapy quickly killed EGFR-expressing cells within minutes after near-infrared light exposure. Photoimmunotherapy induced irreversible cellular membrane damage that allowed extracellular water to enter into cells resulting in swelling, blebbing, and bursting of the cells (6). Although the mechanism of photoimmunotherapy remains unclear, none of the singlet oxygen quenchers or reducing agents, including sodium azide, glutathione, 4-hydroxy-2,2,6,6-tetramethylpiperidin-1-oxyl, etc., interfered with the efficacy of photoimmunotherapy, suggesting a mechanism other than singlet oxygen (type II reaction). However, the actual mechanism of cell membrane injury remains unclear. Because photoimmunotherapy leaves the vasculature intact and the perivascular tumor cells are rapidly killed by photoimmunotherapy, there is a sudden increase in vascular permeability, especially for larger molecules (10). Nanosized reagents, in this case liposomal daunorubicin, were administered after photoimmunotherapy and homogeneously distributed within the tumor at 5-fold concentrations in the normal tumor based on contralateral nontreated controls. The combination of photoimmunotherapy and liposomal daunorubicin increased the survival of mice compared with either photoimmunotherapy or liposomal daunorubicin alone.

In previous work, EGFR-targeted photoimmunotherapy using panitumumab–IR700 with repeated near-infrared light exposures was able to cure >80% of A431 tumors with photoimmunotherapy alone (11). However, an unrealistic feature of this model is that the monoclonal A431 cells homogeneously expressed high levels of EGFR, whereas most tumors contain mixtures of antigen-positive and antigen-negative cells. Therefore, the mixed tumor model described here, which contains both EGFR-positive A431 and EGFR-negative Balb/DsRed

Published OnlineFirst December 19, 2013; DOI: 10.1158/1535-7163.MCT-13-0633

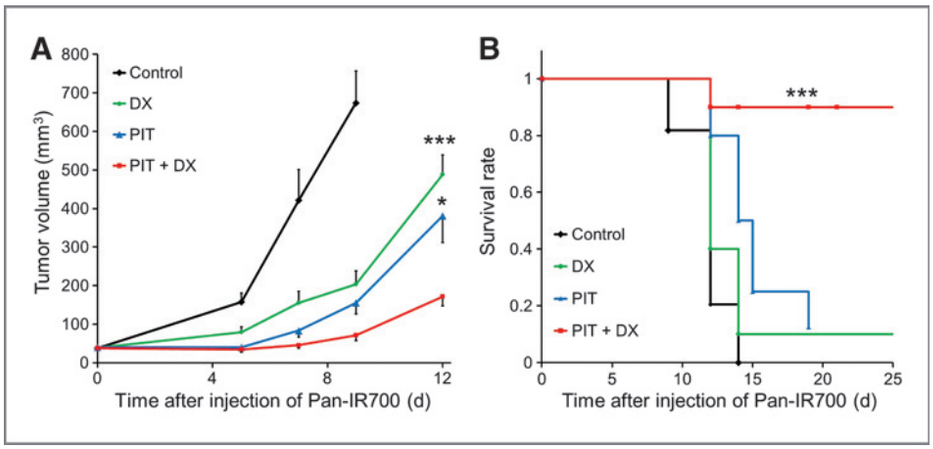

Figure 3. *In vivo* therapeutic effect induced by the combination of PIT and liposomal daunorubicin. A, tumor growth inhibition by a combination therapy of Pan-IR700–mediated PIT and liposomal daunorubicin in A431 and Balb/DsRed tumors. Data, mean ± SEM; $n \geq 10$ mice in each group; ***, $P < 0.01$; *, $P < 0.05$ for treatment compared with DX-only groups and PIT-only groups. B, analysis using a Kaplan–Meier survival curve of the combination therapy of PIT and liposomal daunorubicin in A431 and Balb/DsRed tumors. Of note, $n \geq 10$ mice in each group; ***, $P < 0.05$ for treatment compared with the other control groups using a log-rank test with a Bonferroni correction for multiple comparisons.

cells, provides more insight into how actual tumors might respond to photoimmunotherapy and how they might be treated with adjuvant liposomal chemotherapies. In this work, we demonstrate that, in contrast with a clonal xenograft model, the mixed tumor model responds better to a combination of therapies rather than photoimmunotherapy or liposomal cancer therapy alone.

Photoimmunotherapy can kill the majority of target-positive cells; however, target-negative cells will be unaffected. Eventually, regrowth will occur with antigen-negative cells. However, photoimmunotherapy induces a SUPR effect that preferentially allows the accumulation of nanosized reagents in the tumor bed. In photoimmunotherapy, the layers of tumor cells adjacent to tumor vessels are killed first, while the endothelial cells are undamaged, leading to intact but dilated vessels that are highly permeable (10). This effectively targets nonspecific nanosized reagents to the remaining target-negative tumor cells. We demonstrate a 5-fold increase in liposomal daunarubicin concentration within photoimmunotherapy-treated tumors compared with untreated tumors. This benefit should accrue to any nanosized reagent and is not specific for liposomal daunorubicin. Thus, photoimmunotherapy enables the use of a broad spectrum of nanosized therapies hitherto limited by enhanced permeability and retention (EPR) effects that are on the order of 1.1- to 1.5-fold higher than background. Scattered cancer cells generally are more susceptible to cancer treatments as the most common barriers to drug delivery are reduced. Thus, the SUPR effect following photoimmunotherapy offers opportunities for the utilization of more nanosized reagents than are currently in use. Therefore, combining photoimmunotherapy and nanosized reagents is theoretically a highly complementary approach for heterogeneous tumors, including treatment of cancer stem–like cells.

A potential alternative would be to use fluorescent proteins, which are excellent endogenous fluorescence emitters and/or singlet oxygen producers. Potentially these could be used for depicting various biologic processes or for killing fluorescent protein–expressing cells, respectively, both *in vitro* and *in vivo*. Another recently reported technology is the use of telomerase promoter–regulated expression of various fluorescent proteins, which are induced with adenovirus-mediated gene transfection *in vivo* (12–15). However, the requirement for virus-mediated *in vivo* gene transfection, makes it unlikely to be translated for human use in the near term. In contrast, the photoimmunotherapy technology described here should be readily translatable as it requires the injection of an antibody–IR700 conjugate and exposure to nonthermal levels of near-infrared light.

It has been reported that conventional photodynamic therapy can also enhance the delivery of various nanosized or macromolecular drugs up to 3-fold compared with control tumor between 0 and 12 hours after photodynamic therapy depending on the dose (16–18). Photosensitizers, including verteporfin, show preferential retention in the tumor vasculature and tumor cells. Histologic analysis did not clearly explain the enhanced drug delivery. However, the preponderance of reports suggests that photodynamic therapy destroys morphologic changes on endothelial cells (18) or the structure of tumor vasculature (16), leading to a transient enhancement of tumor vasculature permeability after low doses of photosensitizer and light exposures with appropriate intervals. The enhanced permeability induced by conventional photodynamic therapy seems to be a dynamic process; therefore, the effective dose of photodynamic therapy usually damages both tumor and vascular cells, resulting in reductions in blood flow (19, 20), which enhances its antitumor effects. In contrast, in photoimmunotherapy, antibody–IR700 conjugates selectively bind to target-positive tumor cells with minimal nontarget cell

Published OnlineFirst December 19, 2013; DOI: 10.1158/1535-7163.MCT-13-0633

uptake of IR700 inducing rapid necrotic damage especially on cancer cells near vessels, thus causing dilatation of tumor vessels and dramatically increasing permeability. We have termed this the SUPR effect, which has been shown to increase the delivery of nanoparticles up to 24-fold compared with control tumors in which only conventional EPR is observed (10). Anti-EGFR antibodies alone did not induce SUPR effects in EGFR-positive tumors. The SUPR effect induced by photoimmunotherapy is not specific for EGFR-expressing tumors but can be seen with a variety of mAb–IR700 conjugates, including anti-HER2-IR700. However, receptor negative cells are unaffected because the hydrophilicity of IR700 prevents binding to cells without the appropriate mAb. When comparing the enhanced permeability with photodynamic therapy with photoimmunotherapy, micro-drug distribution after photodynamic therapy showed that the nanosized drugs were located only near blood vessels (16, 18), whereas after photoimmunotherapy, daunorubicin was homogeneously delivered into both the expressing and nonexpressing parts of the tumor. Therefore, the magnitude of SUPR effects induced by photoimmunotherapy is greater than the enhanced drug delivery after photodynamic therapy.

Conclusion

A mixed tumor model containing EGFR-positive and -negative tumor cells was established to better understand the effects of photoimmunotherapy in heterogeneous cancer cell populations. Although photoimmunotherapy successfully treated EGFR-positive A431 cells, EGFR-negative Balb/DsRed cells were not responsive and eventually became the dominant cell. However, photoimmunotherapy also induced a large increase in tumor permeability (also known as the SUPR effect), which allowed a 5-fold increase in the accumulation of an adjuvant liposomal chemotherapy (DaunoXome) and resulted in more effective therapy than either photoimmunotherapy or liposomal daunorubicin alone. The liposomal daunorubicin administered 1 hour after EGFR-targeted photoimmunotherapy was homogeneously distributed, allowing delivery to and killing of EGFR-negative Balb/DsRed cells, resulting in prolonged survival of mice.

Disclosure of Potential Conflicts of Interest

No potential conflicts of interest were disclosed.

Authors' Contributions

Conception and design: P.L. Choyke, H. Kobayashi
Development of methodology: H. Kobayashi
Acquisition of data (provided animals, acquired and managed patients, provided facilities, etc.): K. Sano, T. Nakajima, H. Kobayashi
Analysis and interpretation of data (e.g., statistical analysis, biostatistics, computational analysis): K. Sano, P.L. Choyke, H. Kobayashi
Writing, review, and/or revision of the manuscript: K. Sano, P.L. Choyke, H. Kobayashi
Administrative, technical, or material support (i.e., reporting or organizing data, constructing databases): T. Nakajima, P.L. Choyke, H. Kobayashi
Study supervision: P.L. Choyke, H. Kobayashi

Grant Support

This research was supported by the Intramural Research Program of the NIH, National Cancer Institute, Center for Cancer Research.

The costs of publication of this article were defrayed in part by the payment of page charges. This article must therefore be hereby marked *advertisement* in accordance with 18 U.S.C. Section 1734 solely to indicate this fact.

Received August 9, 2013; revised November 26, 2013; accepted December 5, 2013; published OnlineFirst December 19, 2013.

References

1. Fidler IJ, Kripke ML. Metastasis results from preexisting variant cells within a malignant tumor. Science 1977;197:893–5.
2. Fidler IJ, Hart IR. Biological diversity in metastatic neoplasms: origins and implications. Science 1982;217:998–1003.
3. Nowell PC. Mechanisms of tumor progression. Cancer Res 1986;46:2203–7.
4. Baylin SB, Jones PA. A decade of exploring the cancer epigenome–biological and translational implications. Nat Rev Cancer 2011;11:726–34.
5. Bissell MJ, Hines WC. Why don't we get more cancer? A proposed role of the microenvironment in restraining cancer progression. Nat Med 2011;17:320–9.
6. Mitsunaga M, Ogawa M, Kosaka N, Rosenblum LT, Choyke PL, Kobayashi H. Cancer cell-selective *in vivo* near infrared photoimmunotherapy targeting specific membrane molecules. Nat Med 2011;17:1685–91.
7. Koyama Y, Hama Y, Urano Y, Nguyen DM, Choyke PL, Kobayashi H. Spectral fluorescence molecular imaging of lung metastases targeting HER2/neu. Clin Cancer Res 2007;13:2936–45.
8. Barrett T, Koyama Y, Hama Y, Ravizzini G, Shin IS, Jang BS, et al. *In vivo* diagnosis of epidermal growth factor receptor expression using molecular imaging with a cocktail of optically labeled monoclonal antibodies. Clin Cancer Res 2007;13:6639–48.
9. Giard DJ, Aaronson SA, Todaro GJ, Arnstein P, Kersey JH, Dosik H, et al. *In vitro* cultivation of human tumors: establishment of cell lines derived from a series of solid tumors. J Natl Cancer Inst 1973;51:1417–23.
10. Sano K, Nakajima T, Choyke PL, Kobayashi H. Markedly enhanced permeability and retention effects induced by photo-immunotherapy of tumors. ACS Nano 2013;7:717–24.
11. Mitsunaga M, Nakajima T, Sano K, Choyke PL, Kobayashi H. Near-infrared theranostic photoimmunotherapy (PIT): repeated exposure of light enhances the effect of immunoconjugate. Bioconjug Chem 2012;23:604–9.
12. Kimura H, Lee C, Hayashi K, Yamauchi K, Yamamoto N, Tsuchiya H, et al. UV light killing efficacy of fluorescent protein-expressing cancer cells *in vitro* and *in vivo*. J Cell Biochem 2010;110:1439–46.
13. Tsai MH, Aki R, Amoh Y, Hoffman RM, Katsuoka K, Kimura H, et al. GFP-fluorescence-guided UVC irradiation inhibits melanoma growth and angiogenesis in nude mice. Anticancer Res 2010;30:3291–4.
14. Momiyama M, Suetsugu A, Kimura H, Kishimoto H, Aki R, Yamada A, et al. Fluorescent proteins enhance UVC PDT of cancer cells. Anticancer Res 2012;32:4327–30.
15. Momiyama M, Suetsugu A, Kimura H, Kishimoto H, Aki R, Yamada A, et al. Imaging the efficacy of UVC irradiation on superficial brain tumors and metastasis in live mice at the subcellular level. J Cell Biochem 2013;114:428–34.
16. Gil M, Bieniasz M, Seshadri M, Fisher D, Ciesielski MJ, Chen Y, et al. Photodynamic therapy augments the efficacy of oncolytic vaccinia virus against primary and metastatic tumours in mice. Br J Cancer 2011;105:1512–21.
17. Snyder JW, Greco WR, Bellnier DA, Vaughan L, Henderson BW. Photodynamic therapy: a means to enhanced drug delivery to tumors. Cancer Res 2003;63:8126–31.

Published OnlineFirst December 19, 2013; DOI: 10.1158/1535-7163.MCT-13-0633

18. Chen B, Pogue BW, Luna JM, Hardman RL, Hoopes PJ, Hasan T. Tumor vascular permeabilization by vascular-targeting photosensitization: effects, mechanism, and therapeutic implications. Clin Cancer Res 2006;12:917–23.
19. Standish BA, Lee KK, Jin X, Mariampillai A, Munce NR, Wood MF, et al. Interstitial Doppler optical coherence tomography as a local tumor necrosis predictor in photodynamic therapy of prostatic carcinoma: an *in vivo* study. Cancer Res 2008;68:9987–95.
20. Standish BA, Jin X, Smolen J, Mariampillai A, Munce NR, Wilson BC, et al. Interstitial Doppler optical coherence tomography monitors microvascular changes during photodynamic therapy in a Dunning prostate model under varying treatment conditions. J Biomed Opt 2007;12:034022.

AACR American Association for Cancer Research

Molecular Cancer Therapeutics

The Effect of Photoimmunotherapy Followed by Liposomal Daunorubicin in a Mixed Tumor Model: A Demonstration of the Super-Enhanced Permeability and Retention Effect after Photoimmunotherapy

Kohei Sano, Takahito Nakajima, Peter L. Choyke, et al.

Mol Cancer Ther 2014;13:426-432. Published OnlineFirst December 19, 2013.